Prell, W.L., Wang, P., Blum, P., Rea, D.K., and Clemens, S.C. (Eds.)
Proceedings of the Ocean Drilling Program, Scientific Results Volume 184

9. Oligocene–Miocene Planktonic Foraminifer Biostratigraphy, Site 1148, Northern South China Sea[1]

Qianyu Li,[2,3] Zhimin Jian,[3] and Baohua Li[4]

ABSTRACT

Over 30 first and last occurrence (FO and LO, respectively) planktonic foraminifer datums were recognized from the Oligocene–Miocene section of Ocean Drilling Program (ODP) Site 1148. Most datum levels occur in similar order as, and are by correlation as probably synchronous with, their open-ocean records. Several datum levels represent local bioevents resulting from dissolution and Site 1148's unique paleoceanographic setting in the northern South China Sea. An age of 9.5–9.8 Ma is estimated for the local LO of *Globoquadrina dehiscens* (257 meters composite depth [mcd]), whereas the local LO of *Globorotalia fohsi* s.l. (301 mcd) is projected to be at ~13.0 Ma and the local FO of *Globigerinatella insueta* (367 mcd) is projected to be at ~18.0 Ma.

The combined planktonic foraminifer and nannofossil results indicate that the Oligocene–Miocene section at Site 1148 is not complete. Unconformities up to 2–3 m.y. in duration, occurring at and before the Oligocene/Miocene boundary (OHS1, OHS2, OHS3, and OHS4 = MHS1), are associated with slump deposits between 457 and 495 mcd that signal tectonic instability during the transition from rifting to spreading in the South China Sea. Shorter unconformities of <0.5 m.y. duration that truncate the Miocene section were more likely to have been caused by sea-bottom erosion as well as dissolution. A total of 12 Miocene unconformities, MHS1 through MHS12, are mainly affected by dissolution and an elevated carbonate compensation depth (CCD) during Miocene third-order glaciations recorded in deep-sea positive oxygen isotope Mi glaciation events. Respectively, they fall at ~457 mcd (MHS1 = Mi-1), 407 mcd (MHS2 = Mi-1a), 385 mcd (MHS3 = Mi-1aa),

[1]Li, Q., Jian, Z., and Li, B., 2004. Oligocene–Miocene planktonic foraminifer biostratigraphy, Site 1148, northern South China Sea. *In* Prell, W.L., Wang, P., Blum, P., Rea, D.K., and Clemens, S.C. (Eds.), *Proc. ODP, Sci. Results,* 184, 1–26 [Online]. Available from World Wide Web: <http://www-odp.tamu.edu/publications/184_SR/VOLUME/CHAPTERS/220.PDF>. [Cited YYYY-MM-DD]
[2]Key Laboratory of Marine Geology DoE, Tongji University, Shanghai 200092, People's Republic of China. **qli01@mail.tongji.edu.cn**
[3]School of Earth and Environmental Sciences, The University of Adelaide, Adelaide SA 5005, Australia. Correspondence author: **qianyu.li@adelaide.edu.au**
[4]Nanjing Institute of Geology and Paleontology, Chinese Academy of Sciences, Nanjing 210008, People's Republic of China.

Initial receipt: 19 December 2002
Acceptance: 9 August 2004
Web publication: 15 December 2004
Ms 184SR-220

366 mcd (MHS4 = Mi-1b), 358 mcd (MHS5 = MLi-1), 333 mcd (MHS6 = Mi-2), 318 mcd (MHS7 = MSi-1), 308 mcd (MHS8 = Mi-3), 295 mcd (MHS9 = Mi-4), 288 mcd (MHS10 = Mi-5), 256 mcd (MHS11 = Mi-6), and 250 mcd (MHS12 = Mi-7). The correlation of these unconformities with Mi events indicates that some related driving mechanisms have been operating, causing deepwater circulation changes concomitantly in world oceans and in the marginal South China Sea.

INTRODUCTION

Site 1148, the deepest site drilled during Ocean Drilling Program (ODP) Leg 184, is located at 18°50.169′N, 116°33.939′E. At a water depth of ~3294 m, it lies on the lower continental slope of China, close to the continent/ocean crust boundary (Fig. F1). One of the objectives of Site 1148 was to recover a continuous Oligocene–Miocene sequence of hemipelagic sediments for studying the early paleoclimate history of the South China Sea (SCS) as related to Himalayan–Tibetan uplift and sea level change (Wang, Prell, Blum, et al., 2000).

F1. Site 1148 location, p. 13.

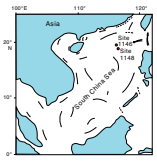

Drilling at Site 1148 recovered a 857-m-long Cenozoic sediment sequence comprising two main sections: a much expanded (mainly lower) Oligocene and the relatively slower accumulated Miocene to Pleistocene. The lower section represents synrift sediments filled during the later Paleogene rifting in half grabens, whereas the upper section corresponds to wider sedimentation during the broad subsidence in the Neogene SCS (Ru et al., 1994; Wang, Prell, Blum, et al., 2000). These two sections are separated by a slumped interval between 457 and 495 meters composite depth (mcd). Imaged as a double reflector in seismic profiles (Wang, Prell, Blum, et al., 2000), the slump may be related to a change in the pattern and direction of seafloor spreading, or "ridge jump" (Briais et al., 1993), which marks the onset of a new tectonic and sedimentological regime beginning in the early Miocene in the SCS region (Wang, Prell, Blum, et al., 2000).

On the basis of initial shipboard data and postcruise results, this study aimed to recover more biostratigraphically useful datums of planktonic foraminifers and to provide a more accurate stratigraphic framework for better dating of Oligocene and Miocene climatic and tectonic events in the region.

SEDIMENT CHARACTERISTICS

The dominant lithology at Site 1148 is clay with variable concentrations of nannofossils. Seven lithostratigraphic units were identified on the basis of composition, depositional facies, and, especially, color variations (Wang, Prell, Blum, et al., 2000). The Pliocene–Holocene is represented by Unit I, the Miocene by Units II–V, and the Oligocene by Unit VI. The main sedimentary characteristics of the Oligocene–Miocene lithostratigraphic units (Units II–VII) are summarized as follows (Wang, Prell, Blum, et al., 2000):

Unit II (194.02–328.82 mcd) is dominated by clay with nannofossils. Light-colored, carbonate-rich layers are frequent, but quartz grains and siliceous microfossils are practically absent. Unit II is defined and subdivided on the basis of color. Olive-gray sediment is found in the upper part of the unit (Subunit IIA, upper

Miocene), and reddish brown sediment composes the lower part of the unit (Subunit IIB, middle to upper Miocene).

Unit III (328.82–360.22 mcd) consists of a grayish green clayey nannofossil ooze with 10- to 50-cm-thick intercalations of dark reddish brown clayey nannofossil ooze or clay with nannofossils. A sudden jump in the chromaticity a* value helps separate Unit III from the underlying unit. This unit is lower middle Miocene.

Unit IV (360.22–412.22 mcd) comprises brownish nannofossil clay mixed sediment with a minor amount of greenish gray nannofossil clay intercalations. Again, the transition across the lithostratigraphic Unit III/IV boundary is marked by a significant increase in the a* value. This unit is lower to lower middle Miocene.

Unit V (412.22–457.22 mcd) mainly consists of greenish gray nannofossil clay mixed sediment interbedded with nannofossil clay and very minor amounts of clay with nannofossils. This unit is lower Miocene.

Unit VI (457.22–494.92 mcd) is the slump deposit, dominantly clay nannofossil mixed sediment and nannofossil clay that resulted from episodic gravitational redeposition, including mass flows and slumping. This unit is upper Oligocene to lower Miocene. Note that the present study identifies the typical slumping interval from 457 to 472 mcd.

Unit VII (494.92–859.45 mcd) is an intensely bioturbated sequence of monotonous grayish olive-green nannofossil clay. It represents the first continuous hemipelagic sedimentation in the SCS during the early and late Oligocene (Wang, Prell, Blum, et al., 2000).

MATERIAL AND METHODS

A total of ~700 samples collected from 170 to 850 mcd at Site 1148 were examined for planktonic foraminifers. Sample spacing varies from 10 to 50 cm and is mostly between 30 and 40 cm unless core recovery was poor.

Samples were processed with standard techniques. Residue >63 µm was collected and separated into two fractions using a 150-µm sieve. The >150-µm fraction was examined using the species concept of Blow (1979), Kennett and Srinivasan (1983), and Bolli and Saunders (1985). The P- and N-zonation scheme developed by Blow (1979) and modified by Berggren et al. (1995) was adopted, and ages for species datums were mainly adopted from Berggren et al. (1995) and Chaisson and Pearson (1997), as summarized in Wang, Prell, Blum, et al. (2000) (Fig. **F2**). Species ranges that were found to be shorter at Site 1148 than in the open ocean are considered local ranges. Table **T1** and Figure **F3** list the observation results, and Figures **F4** and **F5** summarize the stratigraphic range of most species at Site 1148.

F2. Zonation and age of datum levels for Site 1148 biostratigraphy, p. 14.

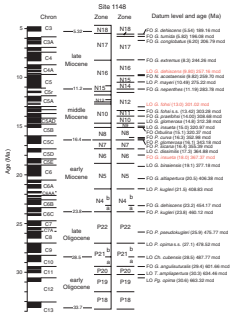

T1. Distribution of Miocene planktonic foraminifers, Site 1148, p. 23.

F3. Oligocene planktonic foraminifer distribution, p. 15.

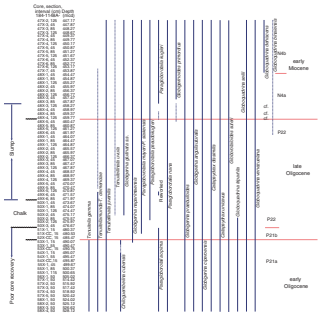

F4. Miocene planktonic foraminifer ranges, p. 16.

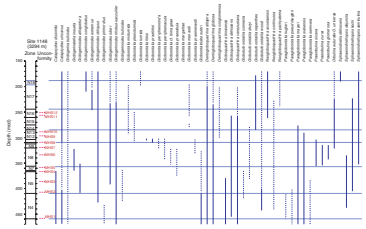

F5. Oligocene planktonic foraminifer ranges, p. 17.

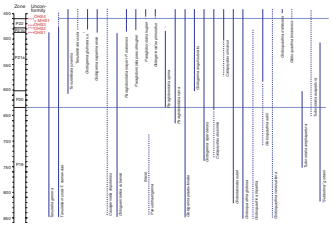

RESULTS

Preservation and General Features of Planktonic Foraminifers

As the Site 1148 locality lies between the modern lysocline (~3000 m) and the carbonate compensation depth (CCD; ~3500 m) (Wang, Prell, Blum, et al., 2000), all calcareous components in the sediment have been affected at least partially by dissolution. The <150-µm residue contains more fragmented planktonic foraminifer tests than the coarser fraction. When few tests are left in the >150-µm residue, the entire finer fraction often contains 100% finely fragmented pieces or is barren. The most severely affected intervals are found at 272–295, 347–349, and 360 mcd, in the middle and upper Miocene. Therefore, the composition as well as species abundance of planktonic foraminifers could have been altered.

The biofacies is dominated by dissolution-resistant species, especially *Sphaeroidinellopsis* spp. and *Globoquadrina* spp. Frequent to abundant taxa include *Globigerinoides, Globoturborotalita, Paragloborotalia, Neogloboquadrina*, and *Catapsydrax*. Others are rare, except in a few short intervals.

Five assemblages can be recognized on the basis of dominant species and species having a shorter range. Because many dissolution-resistant species range through several time periods, these assemblages are only loosely defined for characterizing the altered planktonic foraminifer fauna found at Site 1148. Their main features are briefly described below.

1. The *Sphaeroidinellopsis seminulina–Globoturborotalita nepenthes* assemblage characterizes the upper Miocene Zones N14–N18 between 190 and 275 mcd. Dominated by *S. seminulina*, this assemblage includes many Neogene globigerinid forms, especially *Globigerinoides obliquus, Globigerinoides sacculifer* s.l., *Globigerinoides ruber*, *Globigerinoides conglobatus*, *G. nepenthes, Globoturborotalita druryi*, *Globoquadrina altispira*, *Globoquadrina globosa*, *Neogloboquadrina acostaensis, Globorotalia menardii,* and *Orbulina*.
2. The *G. altispira–S. seminulina–Orbulina* assemblage between 275 and 358 mcd is from the middle Miocene Zones N8–N12. Numerous *Globoquadrina, Sphaeroidinellopsis,* and *Paragloborotalia mayeri–Paragloborotalia siakensis* characterize this assemblage, together with the *Praeorbulina–Orbulina* bioseries. Several globorotaliid lineages are also confined to this assemblage interval, including the *Globorotalia peripheroronda–Globorotalia fohsi* and *Globorotalia praescitula–Globorotalia praemenardii* lineages.
3. The *G. globosa–Sphaeroidinellopsis kochi* assemblage characterizes the lower Miocene Zones N4–N11 between 358 and 454 mcd. Apart from these two species, several related species are also common, including *Globoquadrina dehiscens, Globoquadrina venezuelana, G. altispira,* and *Sphaeroidinellopsis disjuncta*. Species of *Globigerinoides, Paragloborotalia, Globorotaloides, Globoturborotalita,* and *Catapsydrax* are few to abundant, depending on their detailed stratigraphic position. Numerous phosphate or algal flakes are present in some samples in which planktonic foraminifers are rare.

4. The *G. venezuelana–Paragloborotalia pseudokugleri* assemblage characterizes the upper Oligocene Subzone P21b and Zone P22 from 454 to 488 mcd. Also frequently occurring are such species as *Catapsydrax dissimilis, Globorotaloides suteri, Globoquadrina sellii, Globigerina ciperoensis, Paragloborotalia nana*, and *Paragloborotalia opima* (P21b).
5. The lower Oligocene *Chiloguembelina cubensis* assemblage below 488 mcd is characterized by *C. cubensis, P. nana–P. opima, Globoquadrina tripartita, G. ciperoensis, Catapsydrax, G. suteri* and many tenuitellid forms. High sedimentation rate in this interval diluted the abundance of planktonic foraminifers in most samples.

Datum Levels and Zones

Figures F4 and F5 illustrate the stratigraphic range of most planktonic foraminifer species in the Oligocene–Miocene section of Site 1148 on the basis of observation results (Table T1; Fig. F3). More than 30 datum levels were selected to define the stratigraphy (Tables T2, T3). The consistent sequential pattern demonstrates that these datum levels are in similar order as from the open ocean and presumably synchronous with the age estimates by Berggren et al. (1995), Chaisson and Pearson (1997), and Pearson and Chaisson (1997). Supporting evidence comes from correlation with nannofossil events identified by Xin Su (pers. comm., 2002) (Table T4). At least three planktonic foraminifer datums, however, appear to represent local bioevents, and they are discussed briefly below.

G. dehiscens is found in and below Sample 184-1148A-27X-4, 90–92 cm (257.23 mcd), although the related species *G. altispira* and *G. venezuelana* range throughout the studied interval. The last occurrence (LO) of *G. dehiscens* has been reported to fall between 5.6 and 6.6 Ma from tropical regions (Spencer-Cervato et al., 1994; Berggren et al., 1995; Chaisson and Pearson, 1997). At Site 1148, it lies ~2.4 m above the first occurrence (FO) of *N. acostaensis* (259.63 mcd) and 14 m below the FO of *Globigerinoides extremus* (244.18 mcd). Respectively, the latter two datums have been estimated to be ~10 Ma (Chaisson and Pearson, 1997) and 8.3 Ma (Berggren et al., 1995). Several other planktonic foraminifer and nannofossil datums also occur within the interval between 240 and 280 mcd (Table T3). The most important are the LOs of *Discoaster hamatus* at 256.37 mcd (9.40 Ma) and *Catinaster calyculus* at 261.81 mcd (9.64 Ma). Therefore, the LO of *G. dehiscens* at 257.23 mcd may bear an age not younger than 9.5 Ma. It could be slightly older, up to ~10 Ma, if an older age of 10.3 Ma (Chaisson and Pearson, 1997) for the FO of *G. extremus* was followed, but the existence of several younger planktonic foraminifer and nannofossil datums below the *G. extremus* level indicates that the age given by Chaisson and Pearson (1997) may not be valid, at least for Site 1148. The LO of *G. dehiscens* at ~10 Ma in planktonic foraminifer Zone N16 has also been recorded from other SCS localities including Sites 1143 and 1146 (Wang, 2001) and many offshore industrial wells (Qin, 1996), indicating a regional event.

The LO of *G. fohsi* at 301.03 mcd marks a sudden disappearance of all related species, and it is apparently truncated by dissolution-related unconformity at ~13 Ma. At Site 1146, this datum appears to be synchronous with its open-ocean record of 11.68 Ma (Wang, 2001).

The FO of *Globigerinatella insueta* at 367.30 mcd is projected to be at ~18.0 Ma, between the much older LO of *Globoquadrina binaiensis* (19.1 Ma; 377 mcd) and slightly younger LO of *C. dissimilis* (17.3 Ma; 365.03

T2. Oligocene–Miocene planktonic foraminifer datum levels, Site 1148, p. 24.

T3. Dating Miocene planktonic foraminifer zonal boundaries, p. 25.

T4. Datum levels used for plotting Figure F7, p. 26.

mcd). Pearson and Chaisson (1997) found the FO of *G. insueta* s.s. at 17.4 Ma in cores from the Ceara Rise. The occurrence of these three datums from 19.1 to 17.3 Ma in an interval of 12 m (365–377 mcd) indicates a condensed section that is probably caused by unconformities.

On the basis of the planktonic foraminifer datum levels given in Table T2, the Oligocene Zones P18–P22 and Miocene Zones N4–N18 can be recognized (Figs. F6, F7). We used the zonation scheme and age estimates by Berggren et al. (1995) for the Oligocene–Miocene section. Age adjustment on the basis of Chaisson and Pearson (1997) has been made for several datums that define the upper middle and upper Miocene zones. As indicated in Figure F2 and Table T3, 9 of the 15 Miocene zonal boundaries are affected by the adjustment, with the Zone N10/N11 boundary registering the biggest difference of 1.3 Ma (12.7–14.0 Ma) (Table T3). Zones N12 and N13 cannot be divided at Site 1148 because the nominated datum, the LO of *G. fohsi*, is truncated by an unconformity.

Therefore, the Pliocene/Miocene boundary is now placed close to 188 mcd on the basis of the FO of *Sphaeroidinella dehiscens* (5.54 Ma), very close to the lithostratigraphic Unit I/II boundary. The upper/middle Miocene boundary falls close to 275 mcd where the FO of *Globoturborotalita nepenthes* (11.19 Ma) also occurs, about 23 m below the Subunit IIA/IIB boundary. The middle/lower Miocene boundary at 355 mcd is defined by the FO of *Praeorbulina sicana* (16.4 Ma), close to the Unit III/IV contact (360 mcd). The Miocene/Oligocene boundary lying at ~460 mcd within the slump is indicated by the FO of *Paragloborotalia kugleri,* only ~3 m below the Unit V/VI boundary. The upper/lower Oligocene boundary is placed at 488 mcd by the LO of *C. cubensis* (28.5 Ma), ~7 m above the lithostratigraphic Unit VI/VII contact. The LO of *Pseudohastigerina* (32 Ma) at ~697 mcd is the oldest planktonic foraminifer datum found at Site 1148, marking the top of Zone P18. This taxon, however, occurs sporadically in the much expanded lower Oligocene section from the bottom part of the core. Nannofossil results indicate that the oldest sediment recovered at 857 mcd of Site 1148 could bear an age of ~33 Ma because the LOs of *Reticulofenestra umbilicus* and *Reticulofenestra hillae* were found at ~730 mcd, both indicating 32.3 Ma (Xin Su, pers. comm., 2002).

Stratigraphic Correlation with Other SCS Localities

An Oligocene–Miocene succession similar to that described here for Site 1148 also occurs in other parts of the SCS. For example, Wang et al. (1981) and Qin (1996) reported Oligocene–Pliocene planktonic foraminifers in several northern SCS basins. Based on sidewall cores and cuttings, however, these studies generate very limited biostratigraphic and paleoceanographic information. A high-resolution biostratigraphy for sediment sequences from the northern continental shelf of the SCS is still lacking.

Miocene and younger sediments were also recovered at Site 1146 during Leg 184. Lying above the lysocline, in a water depth of 2092 m, Site 1146 provides much better preserved material with considerably less dissolution than at Site 1148 (Wang, 2001). Figure F7 attempts a correlation between these two sites based on planktonic foraminifer zones identified. Clearly, the middle and upper Miocene sections at these two sites are relatively complete, as represented by Zones N8–N18. A thinner middle to upper Miocene section at Site 1148, ~160 m, compared to 270 m at Site 1146, is interpreted mainly due to its remote

F6. Upper Oligocene unconformity determination, p. 18.

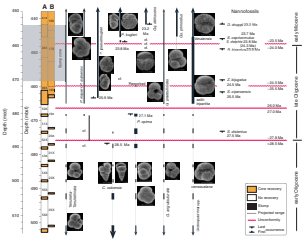

F7. Site 1146 and 1148 correlation, planktonic foraminifer zonation, and unconformities, p. 19.

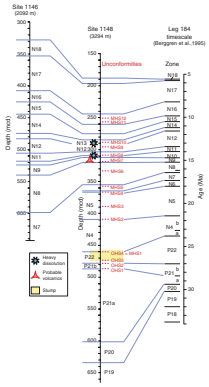

locality and a greater water depth where sedimentation rates were lower and dissolution was stronger (Fig. F7).

Abundant reddish planktonic foraminifers were preserved between 314 and 316 mcd at Site 1148. Together with some volcanic remnants, they probably indicate a period of strong local volcanism at ~14.8 Ma. Further studies are needed to clarify this.

DISCUSSION

Unconformities and Dissolution Events

Figure F8 illustrates planktonic foraminifer and nannoplankton datum levels, as well as the calculated sedimentation rates and unconformities found at Site 1148. Very high sedimentation rates of >100 m/m.y. account for the accumulation during rifting of the exceptionally thick lower Oligocene section, whereas the Miocene sediments were deposited during relatively stable seafloor spreading periods at moderate rates of 15–30 m/m.y. The 457- to 495-mcd interval, including the slump, marks the transition from rifting to stable spreading of the SCS (Briais et al., 1993; Wang, Prell, Blum, et al., 2000; Li et al., 2003). It is not clear, however, how this major tectonic event in the regional West Pacific affected paleoceanography of other regions where a more complete sediment record exists (e.g., Pacific: Kroenke et al., 1993; Atlantic: Flower et al., 1997; Mutti, 2000; Subantarctic: Billups et al., 2002).

At least four major unconformities are present in the upper Oligocene (Fig. F6), respectively, at ~488 mcd (OHS1), ~478 mcd (OHS2), 472 mcd (OHS3), and 460 mcd (OHS4). OHS1 at 488 mcd coincides with the lower/upper Oligocene boundary and represents a break of at least 0.5 m.y., based on the LO of *C. cubensis* (28.5 Ma) at 487.77 mcd and the LO of *Sphenolithus distentus* (27.7 Ma) at 485.34 mcd. It is also marked by the most pronounced changes in all physical property records (Wang, Prell, Blum, et al., 2000) (Fig. F9). OHS2 is indicated by the sudden disappearance of *P. opima* at ~478 mcd (27.1 Ma) and by the FO of *P. pseudokugleri* (25.9 Ma) from only ~3 m above this level, suggesting a hiatus of ~1 m.y. (between 26.0 and 27.0 Ma). OHS3 and OHS4 lie within the slump between 457 and 472 mcd, although the whole interval can be collectively considered as representing a single unconformity if the slump deposition had occurred in a very short period of time rather than during the entire period of ~23.4–25.4 Ma. Different lithofacies and biofacies distinguish two slumped packages, between 458 and 460 mcd and between 460 and 472 mcd, that correspond to two slumping epochs, each footing on an unconformity surface. Although no microfossil events were observed directly at the 472-mcd level (OHS3), the LO of *Sphenolithus ciperoensis* (25.5 Ma) at 474 mcd and the LO of *Zygrhablithus bijugatus* (23.8–24.5 Ma) at 470 mcd suggest a gap at the base of slump would be at least 1 m.y. in duration, between ~24.5 and 25.5 Ma. This is because the 4- to 5-m slumped section between these two datums cannot fully represent a deposition of 1 m.y., even if an error bar of 0.5–1.0 m for the datums was considered. Sediments close to 460 mcd underwent a change in the slumped lithofacies and biofacies, and the presence of two bioevents, the FO of *P. kugleri* (23.8 Ma) and the LO of *Reticulofenestra bisectus* (23.9 Ma), indicates a horizon close to the Oligocene/Miocene boundary coinciding with OHS4. Because the average sedimentation rate during the early Miocene at Site 1148 was ~15 m/m.y. (Fig. F7), we may assume that a

F8. Site 1148 biostratigraphic framework, p. 20.

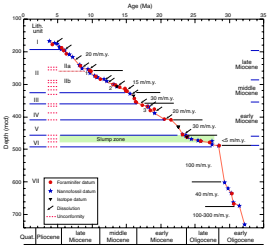

F9. Lithostratigraphic unit boundaries, p. 21.

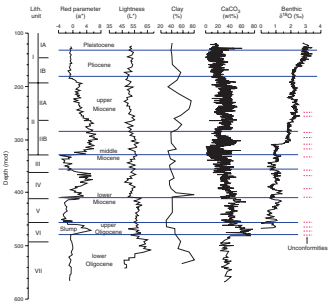

rate at least twice as fast as 15 m/m.y could account for the gravity flow deposition and the lower slumped package between 460 and 478 mcd could represent a <0.5-m.y. deposition between 24.0 and 24.5 Ma. Consequently, the unconformity across the Oligocene/Miocene boundary would be ~0.5 m.y. in duration between 23.5 and 24.0 Ma and the upper slumped package between 458 and 460 would likely accumulate in the first 0.1 m.y. after the boundary unconformity (i.e., at 23.4 Ma). Because the OHS4 event occurred across the Oligocene/Miocene boundary, it is also assigned to represent the first Miocene unconformity event, MHS1.

Although there are no apparent post-Oligocene slumps, 11 surfaces collectively called unconformities MHS2–MHS12 within the relatively complete Miocene section are associated with either some bioevents clustering together and causing shorter and incomplete biozones or with heavy dissolution (Figs. **F7, F8**). The FO of *Globigerinoides altiapertura* (20.5 Ma) at 408 mcd and the LO of *P. kugleri* (21.5 Ma) at 411 mcd indicate a Miocene unconformity MHS2 of at least 0.5 m.y., which includes a dissolution event at ~407 mcd. MHS3–MHS12 also match the dissolution events at 385, 366, 358, 333, 318, 308, 295, 288, 256, and 250 mcd, respectively (Fig. **F8**). Among them, MHS4 and MHS9 erased part of the sediment record for Zones N6 and N10 (Fig. **F7**), whereas others mark sudden changes in various physical property signals that were used for subdividing lithostratigraphic units (Fig. **F9**). Except for those defined by planktonic foraminifer and nannofossil datums, many of these Miocene dissolution events found at Site 1148 and collectively called unconformities may each represent a missing interval of <0.3 m.y.

CCD and Bottom Circulation Changes

The altered planktonic foraminifer assemblage found at Site 1148 was affected by dissolution as a result of lysocline and CCD fluctuations, especially during the Miocene. Few complete tests are preserved in samples affected by strong dissolution, and this pattern occurs repeatedly at certain levels, representing heavy dissolution cycles (Figs. **F8, F9**). This phenomenon is widespread in the tropical western Pacific where the lysocline is elevated (Kennett et al., 1985; Kroenke et al., 1993).

Major dissolution events occurred in the later part of the middle Miocene (~308 and ~288 mcd), apparently corresponding to the "carbonate crash" widely recorded in tropical oceanic settings (Roth et al., 2000). This has been attributed to the formation or strengthening of the Atlantic Deep Water and Antarctic Deep Water, which caused an elevated CCD and strong deep-sea dissolution worldwide (Woodruff and Savin, 1991; Hodell and Woodruff, 1994; Lyle et al., 1995). In addition to these events, at Site 1148 there is a series of smaller-scale dissolution events at ~457, ~407, ~385, ~366, ~358, ~333, ~318, ~295, ~288, ~256, and ~250 mcd, respectively (Fig. **F8**). On the basis of correlation, these dissolution events appear to fall at or close to the positive oxygen isotope Mi events of Miller et al. (1991, 1996, 1998) or the MLi–MSi events of Hardenbol et al. (1998) that signal Miocene glaciations. Specifically, the Miocene dissolution events identified at Site 1148 correspond at least in age to isotopic glaciations Mi-1 (457 mcd), Mi-1a (407 mcd), Mi-1aa (385 mcd), Mi-1b (366 mcd), MLi1 (358 mcd), Mi-2 (333 mcd), MSi1 (318 mcd), Mi-3 (308 mcd), Mi-4 (295 mcd), Mi-5 (288 mcd), Mi-6 (256 mcd), and Mi-7 (250 mcd) (Fig. **F9**). This correlation also implies

that all heavy dissolution observed at Site 1148 was related to a corrosive deep water that was strengthened during major glaciation periods.

A positive relationship between the Miocene dissolution events and Mi glaciations indicates a link to deep-sea watermass changes in the SCS (Fig. F10). Some appear to coincide with deep-sea hiatuses recognized elsewhere by Keller and Baron (1983, 1987) and Keller et al. (1987), although their dissolution origin is still debated (Haq, 1991; Kroenke et al., 1993; Spencer-Cervato, 1998). Apart from those associated with the upper Oligocene slump, most Miocene unconformities found at Site 1148 have been more likely related to dissolution than to local tectonics, although some of them (e.g., MHS4 and MHS8) (Fig. F10) could have been affected also from sediment removal by underwater currents.

F10. Lithobiostragraphic events, p. 22.

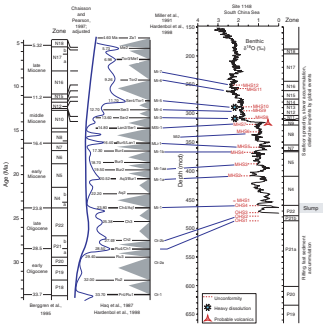

SUMMARY

1. Because the Site 1148 locality now lies between the modern lysocline and CCD in the northern SCS, Oligocene and Miocene planktonic foraminifers from Site 1148 are found to have been affected to a varying extent by dissolution. The biofacies is dominated by dissolution-resistant species, especially *S. seminulina* and *Globoquadrina* spp.
2. More than 30 planktonic foraminifer datum levels are found between 170 and 700 mcd, enabling the recognition of Oligocene Zones P18–P22 and Miocene Zones N4–N18. By correlation, most bioevents are considered synchronous with their open-ocean records. Three of them, however, appear to represent local events: the LO of *G. dehiscens* at ~9.5 Ma, the LO of *G. fohsi* s.l. at ~13.0 Ma, and the FO of *G. insueta* at ~18.0 Ma.
3. At least four major unconformities occurred in the late Oligocene, respectively, at ~488 mcd (OHS1), ~478 mcd (OHS2), 472 mcd (OHS3), and 457 mcd (OHS4 = MHS1). The last two are in the slump deposit between 458 and 472 mcd that marks the transition from rifting to spreading of the SCS.
4. Miocene unconformities MHS1–MHS12 are mainly caused by dissolution because of an elevated CCD during third-order glaciations or Mi events. This positive relationship indicates that a similar or related driving mechanism was responsible for deep-water circulation changes concomitantly in world oceans and the marginal SCS during the Miocene.

ACKNOWLEDGMENTS

This research used samples and/or data provided by the Ocean Drilling Program (ODP). ODP is sponsored by the U.S. National Science Foundation (NSF) and participating countries under management of Joint Oceanographic Institutions (JOI), Inc. Funding for this research was provided by grants from the National Natural Science Foundation of China, Chinese Academy of Sciences, and Australian Research Council. Xin Su supplied unpublished nannofossil data. Oxygen isotopic data and calculation of isotopic events were provided by Quanhong Zhao. William Chaisson and Peter Blum reviewed the manuscript and offered valuable suggestions.

REFERENCES

Berggren, W.A., Kent, D.V., Swisher, C.C., III, and Aubry, M.-P., 1995. A revised Cenozoic geochronology and chronostratigraphy. *In* Berggren, W.A., Kent, D.V., Aubry, M.-P., and Hardenbol, J. (Eds.), *Geochronology, Time Scales and Global Stratigraphic Correlation*. Spec. Publ.—SEPM (Soc. Sediment. Geol.), 54:129–212.

Billups, K., Channell, J.E.T., and Zachos, J.C., 2002. Late Oligocene to early Miocene geochronology and paleoceanography from the subantarctic South Atlantic. *Paleoceanography,* 17:4-1–4-11.

Blow, W.H., 1979. *The Cainozoic Globigerinida:* Leiden (E.J. Brill).

Bolli, H.M., and Saunders, J.B., 1985. Oligocene to Holocene low latitude planktic foraminifera. *In* Bolli, H.M., Saunders, J.B., and Perch-Nielsen, K. (Eds.), *Plankton Stratigraphy:* Cambridge (Cambridge Univ. Press), 155–262.

Briais, A., Patriat, P., and Tapponnier, P., 1993. Updated interpretation of magnetic anomalies and seafloor spreading stages in the South China Sea: implications for the Tertiary tectonics of Southeast Asia. *J. Geophys. Res.,* 98:6299–6328.

Chaisson, W.P., and Pearson, P.N., 1997. Planktonic foraminifer biostratigraphy at Site 925: middle Miocene–Pleistocene. *In* Shackleton, N.J., Curry, W.B., Richter, C., and Bralower, T.J. (Eds.), *Proc. ODP, Sci. Results,* 154: College Station, TX (Ocean Drilling Program), 3–31.

Chen, X., Zhao, Q., and Jian, Z., 2002. Carbonate content changes since the Miocene and paleoenvironmental implications, ODP Site 1148, northern South China Sea. *Haiyang Dizhi Yu Disiji Dizhi,* 22:69–74. (in Chinese)

Flower, B.P., Zachos, J.C., and Martin, E., 1997. Latest Oligocene through early Miocene isotopic stratigraphy and deep-water paleoceanography of the western equatorial Atlantic: Sites 926 and 929. *In* Shackleton, N.J., Curry, W.B., Richter, C., and Bralower, T.J. (Eds.), *Proc. ODP, Sci. Results,* 154: College Station, TX (Ocean Drilling Program), 451–461.

Haq, B.U., 1991. Sequence stratigraphy, sea-level change, and significance for the deep sea. *In* Macdonald, D.I.M. (Ed.), *Sedimentation, Tectonics and Eustasy: Sea Level Changes at Active Margins*. Spec. Publ. Int. Assoc. Sedimentol., 12:3–39.

Haq, B.U., Hardenbol, J., and Vail, P.R., 1987. Chronology of fluctuating sea levels since the Triassic. *Science,* 235:1156–1167.

Hardenbol, J., Thierry, J., Farley, M.B., de Graciansky, P.-C., and Vail, P.R., 1998. Mesozoic and Cenozoic sequence chronostratigraphic framework of European basins. *In* de Graciansky, P.-C., Hardenbol, J., Jacquin, T., and Vail, P.R. (Eds.), *Mesozoic and Cenozoic Sequence Stratigraphy of European Basins*. Spec. Publ.—SEPM (Soc. Sediment. Geol.), 60:3–13, Charts 1–8.

Hodell, D.A., and Woodruff, F., 1994. Variations in the strontium isotopic ratio of seawater during the Miocene: stratigraphic and geochemical implications. *Paleoceanography,* 9:405–426.

Keller, G., and Barron, J.A., 1983. Paleoceanographic implications of Miocene deep-sea hiatuses. *Geol. Soc. Am. Bull.,* 97:590–613.

Keller, G., and Barron, J.A., 1987. Paleodepth distribution of Neogene deep-sea hiatuses. *Paleoceanography,* 2:697–713.

Keller, G., Herbert, T., Dorsey, R., D'Hondt, S., Johnsson, M., and Chi, W.R., 1987. Global distribution of late Paleogene hiatuses. *Geology,* 15:199–203.

Kennett, J.P., Keller, G., and Srinivasan, M.S., 1985. Miocene planktonic foraminiferal biogeography and paleoceanographic development of the Indo-Pacific region. *In* Kennett, J.P. (Ed.), *The Miocene Ocean: Paleoceanography and Biogeography.* Mem.—Geol. Soc. Am., 163:197–236.

Kennett, J.P., and Srinivasan, M.S., 1983. *Neogene Planktonic Foraminifera: A Phylogenetic Atlas:* Stroudsburg, PA (Hutchinson Ross).

Kroenke, L.W., Resig, J.M., and Leckie, R.M., 1993. Hiatus and tephrochronology of the Ontong Java Plateau: correlation with regional tectono-volcanic events. *In*

Berger, W.H., Kroenke, L.W., Mayer, L.A., et al., *Proc. ODP, Sci. Results,* 130: College Station, TX (Ocean Drilling Program), 423–444.

Li, X., Wei, G., Shao, L., Liu, Y., Liang, X., Jian, Z., Sun, M., and Wang, P., 2003. Geochemical and Nd isotopic variations in sediments of the South China Sea: a response to Cenozoic tectonism in SE Asia. *Earth Planet. Sci. Lett.,* 211:207–220.

Lyle, M., Dadey, K.A., and Farrell, J.W., 1995. The late Miocene (11–8 Ma) eastern Pacific carbonate crash: evidence for reorganization of deep-water circulation by the closure of the Panama Gateway. *In* Pisias, N.G., Mayer, L.A., Janecek, T.R., Palmer-Julson, A., and van Andel, T.H. (Eds.), *Proc. ODP, Sci. Results,* 138: College Station, TX (Ocean Drilling Program), 821–838.

Miller, K.G., Mountain, G.S., Browning, J.V., Kominz, M., Sugarman, P.J., Christie-Blick, N., Katz, M.E., and Wright, J.D., 1998. Cenozoic global sea level, sequences, and the New Jersey transect: results from coastal plain and continental slop drilling. *Rev. Geophys.,* 36:569–601.

Miller, K.G., Mountain, G.S., Leg 150 Shipboard Party, and Members of the New Jersey Coastal Plain Drilling Project, 1996. Drilling and dating New Jersey Oligocene–Miocene sequence: ice volume, global sea level, and Exxon records. *Science,* 271:1092–1095.

Miller, K.G., Wright, J.D., and Fairbanks, R.G., 1991. Unlocking the Ice House: Oligocene–Miocene oxygen isotopes, eustasy, and margin erosion. *J. Geophys. Res.,* 96:6829–6848.

Mutti, M., 2000. Bulk $\delta^{18}O$ and $\delta^{13}C$ records from Site 999, Colombian Basin, and Site 1000, Nicaraguan Rise (latest Oligocene to middle Miocene): diagenesis, link to sediment parameters, and paleoceanography. *In* Leckie, R.M., Sigurdsson, H., Acton, G.D., and Draper, G. (Eds.), *Proc. ODP, Sci. Results,* 165: College Station, TX (Ocean Drilling Program), 275–283.

Pearson, P.N., and Chaisson, W.P., 1997. Late Paleocene to middle Miocene planktonic foraminifer biostratigraphy of the Ceara Rise. *In* Shackleton, N.J., Curry, W.B., Richter, C., and Bralower, T.J. (Eds.), *Proc. ODP, Sci. Results,* 154: College Station, TX (Ocean Drilling Program), 33–68.

Qin, G., 1996. Biostratigraphic zonation and correlation of the late Cenozoic planktonic foraminifera in Pearl River Mouth Basin. *In* Hao, Y. (Ed.), *Research on Micropalaeontology and Paleoceanography in Pearl River Mouth Basin, South China Sea:* Beijing (China Univ. Geosci. Press), 19–31. (in Chinese)

Roth, J.M., Droxler, A.W., and Kameo, K., 2000. The Caribbean carbonate crash at the middle to late Miocene transition: linkage to the establishment of the modern global ocean conveyor. *In* Leckie, R.M., Sigurdsson, H., Acton, G.D., and Draper, G. (Eds.), *Proc. ODP, Sci. Results,* 165: College Station, TX (Ocean Drilling Program), 249–273.

Ru, K., Zhou, D., and Chen, H., 1994. Basin evolution and hydrocarbon potential of the northern South China Sea. *In* Zhou, D., Liang, Y., and Zeng, C. (Eds.), *Oceanology of China Seas:* New York (Kluwer Press), 2:361–372.

Spencer-Cervato, C., 1998. Changing depth distribution of hiatuses during the Cenozoic. *Paleoceanography,* 13:178–182.

Spencer-Cervato, C., Thierstein, H.R., Lazarus, D.B., and Beckmann, J.-P., 1994. How synchronous are Neogene marine plankton events? *Paleoceanography,* 9:739–763.

Wang, J., 2001. Planktonic foraminiferal assemblages and paleoceanography during the last 18 Ma—a study on ODP Sites 1146 and 1148, northern South China Sea [Ph.D. thesis]. Tongji Univ.

Wang, P., He, Y., Hu, L., Qin, G., Xia, L., Qiu, S., Lin, J., He, X., Bian, Y., Zheng, F., Cheng, X., Han, Y., and Yao, X., 1981. Foraminifera. *In* Hou, Y. (Ed.), *Atlas of Tertiary Fossils from Northern Continental Shelf of South China Sea:* Guangzhou (Guangdoing Sci. and Technol. Publ.), 83–137. (in Chinese)

Wang, P., Prell, W.L., Blum, P., et al., 2000. *Proc. ODP, Init. Repts.,* 184 [CD-ROM]. Available from: Ocean Drilling Program, Texas A&M University, College Station TX 77845-9547, USA.

Woodruff, F., and Savin, S.M., 1991. Mid-Miocene isotope stratigraphy in the deep-sea: high resolution correlations, paleoclimatic cycles, and sediment preservation. *Paleoceanography,* 6:755–806.

Zhao, Q., Jian, Z., Wang, J., Cheng, X., Huang, B., Xu, J., Zhou, Z., Fang, D., and Wang, P., 2001. Neogene oxygen isotopic stratigraphy, ODP Site 1148, northern South China Sea. *Sci. China, Ser. D.: Earth Sci.,* 44:934–942.

Figure F1. Location of Site 1148 in the northern South China Sea. Major circulation patterns are indicated.

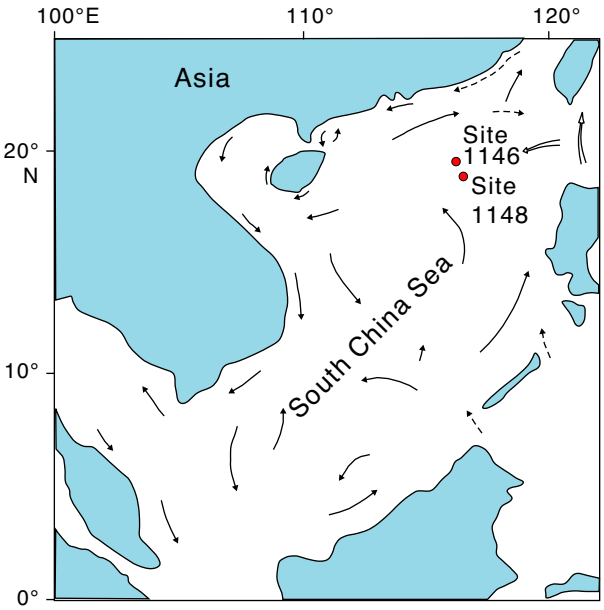

Figure F2. Zonation and age of datum levels by Berggren et al. (1995) (right) and those by Chaisson and Pearson (1997) and Pearson and Chaisson (1997) (left) are adopted for Site 1148 biostratigraphy. FO = first occurrence, LO = last occurrence. Red = three local datum levels.

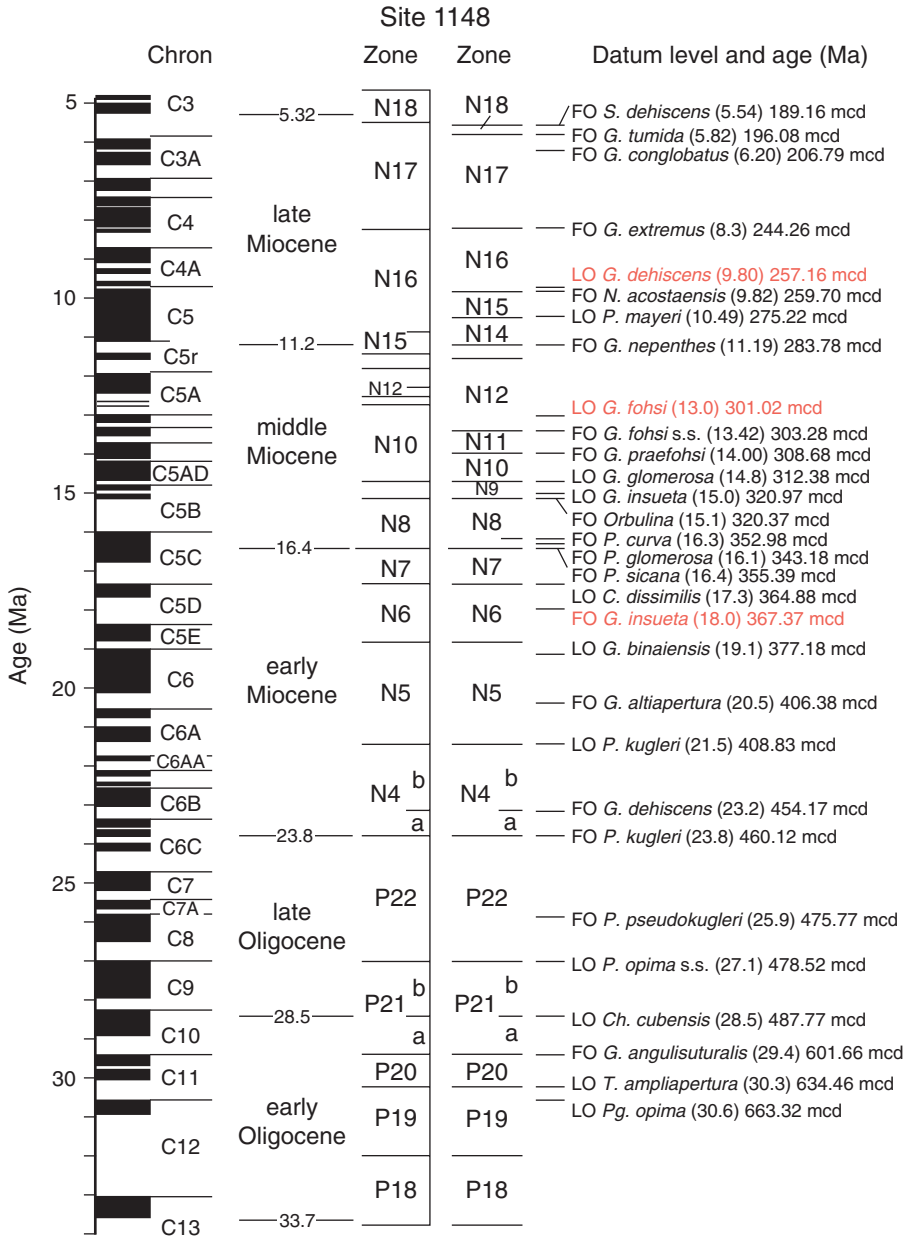

Figure F3. Distribution of Oligocene planktonic foraminifers, Site 1148.

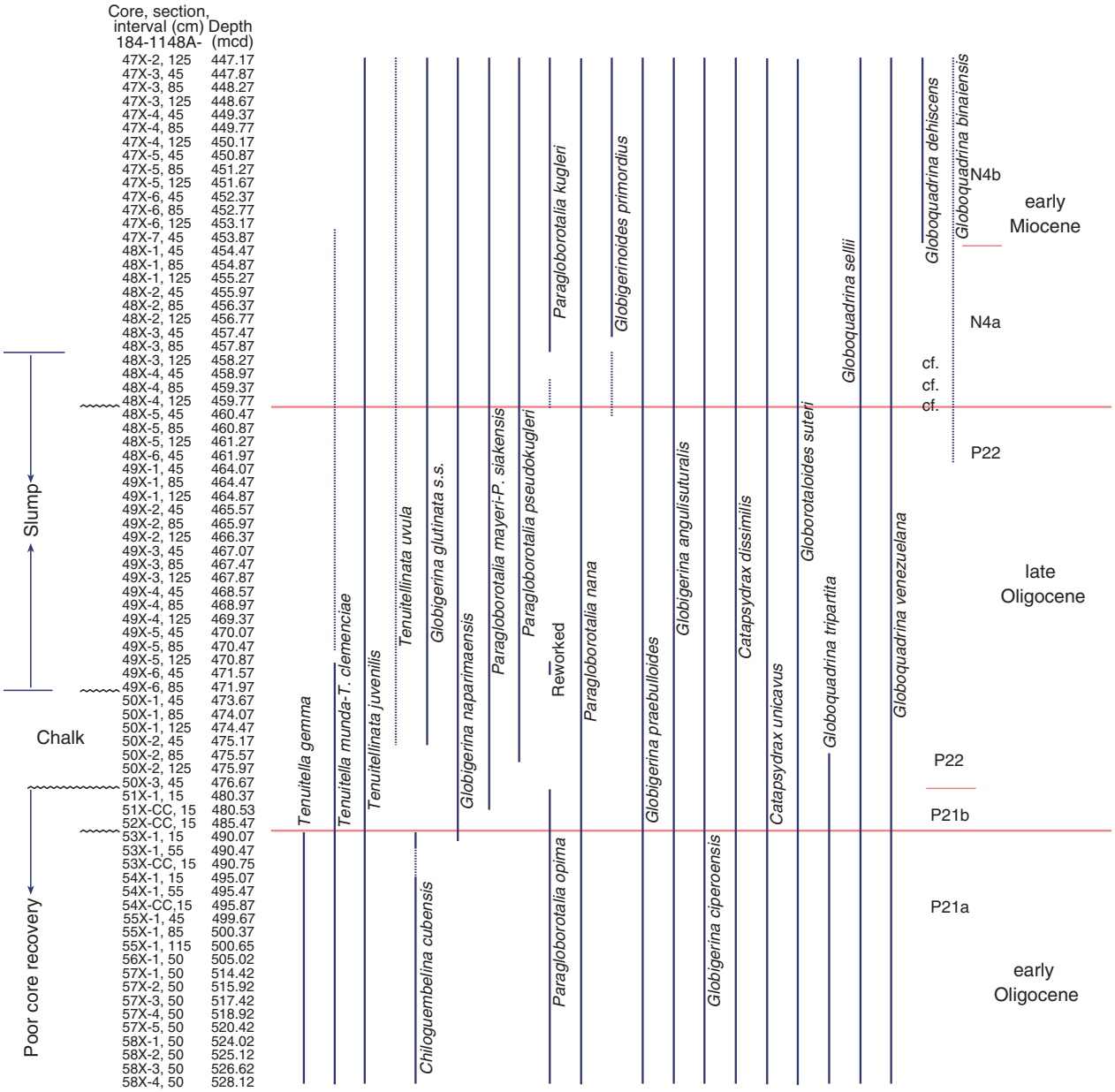

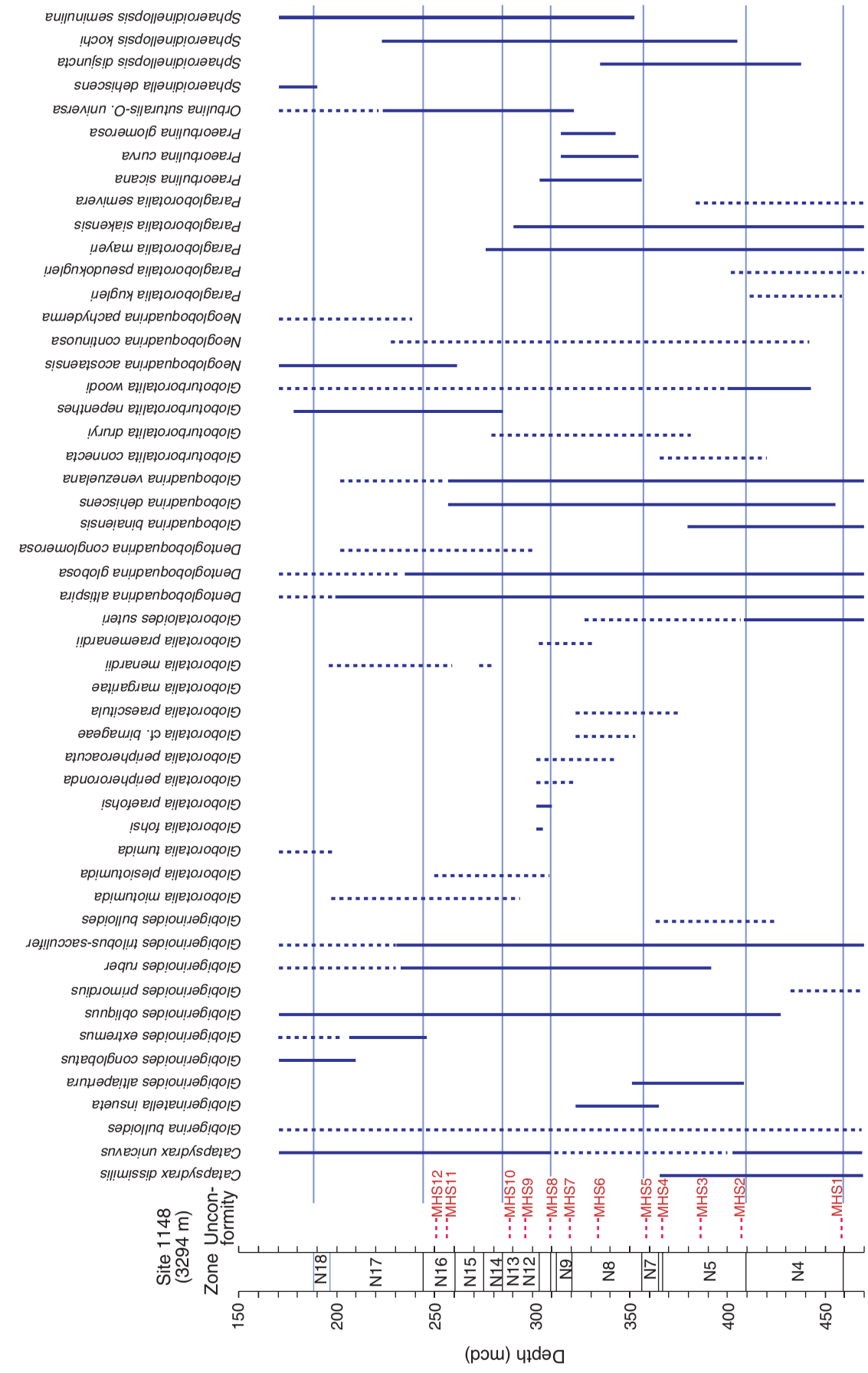

Figure F4. Ranges of planktonic foraminifers in the Miocene section of Site 1148. Bold lines = common occurrences, dashed lines = rare occurrences.

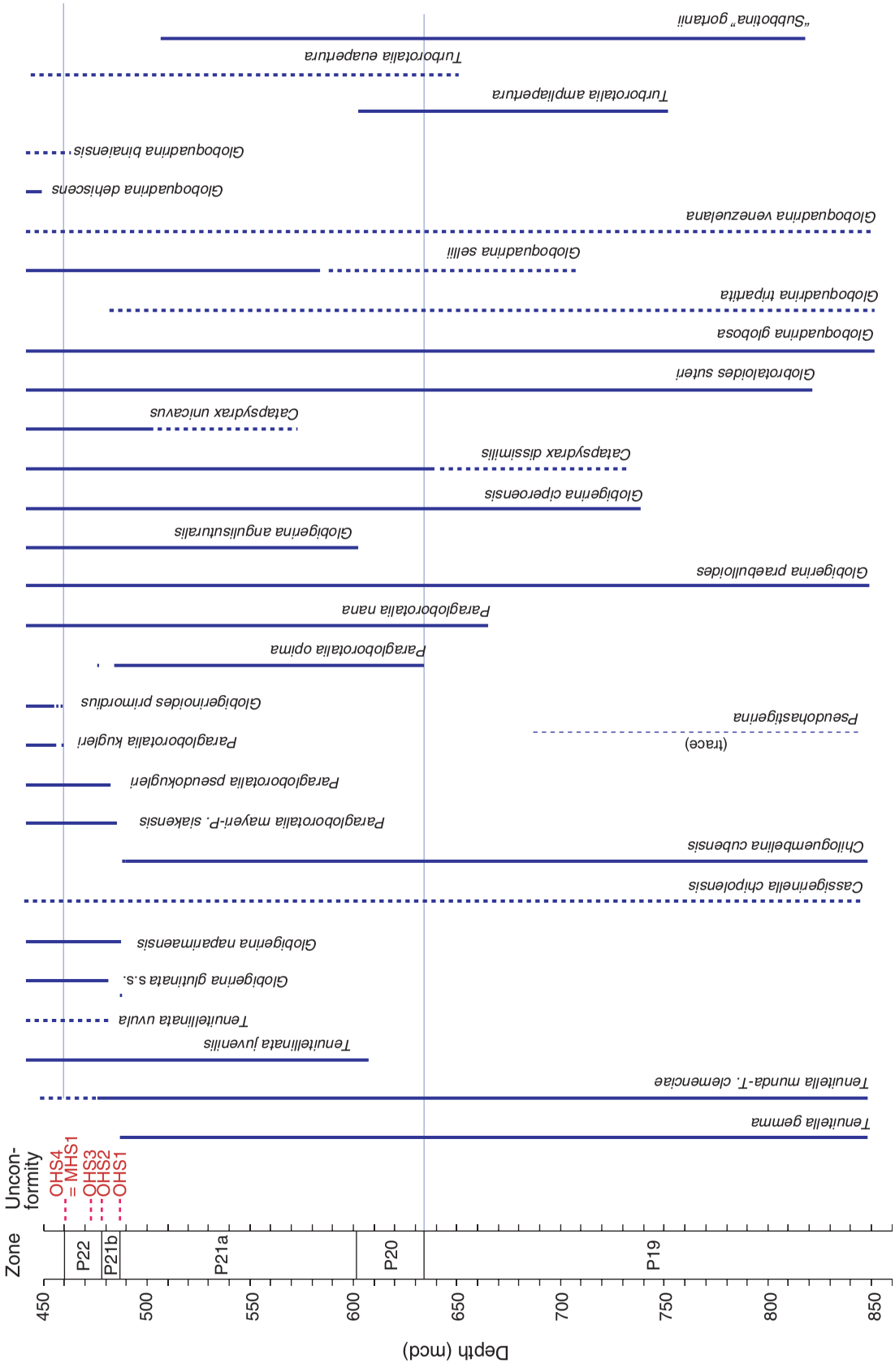

Figure F5. Ranges of planktonic foraminifers in the Oligocene section of Site 1148. Bold lines = common occurrences, dashed lines = rare occurrences.

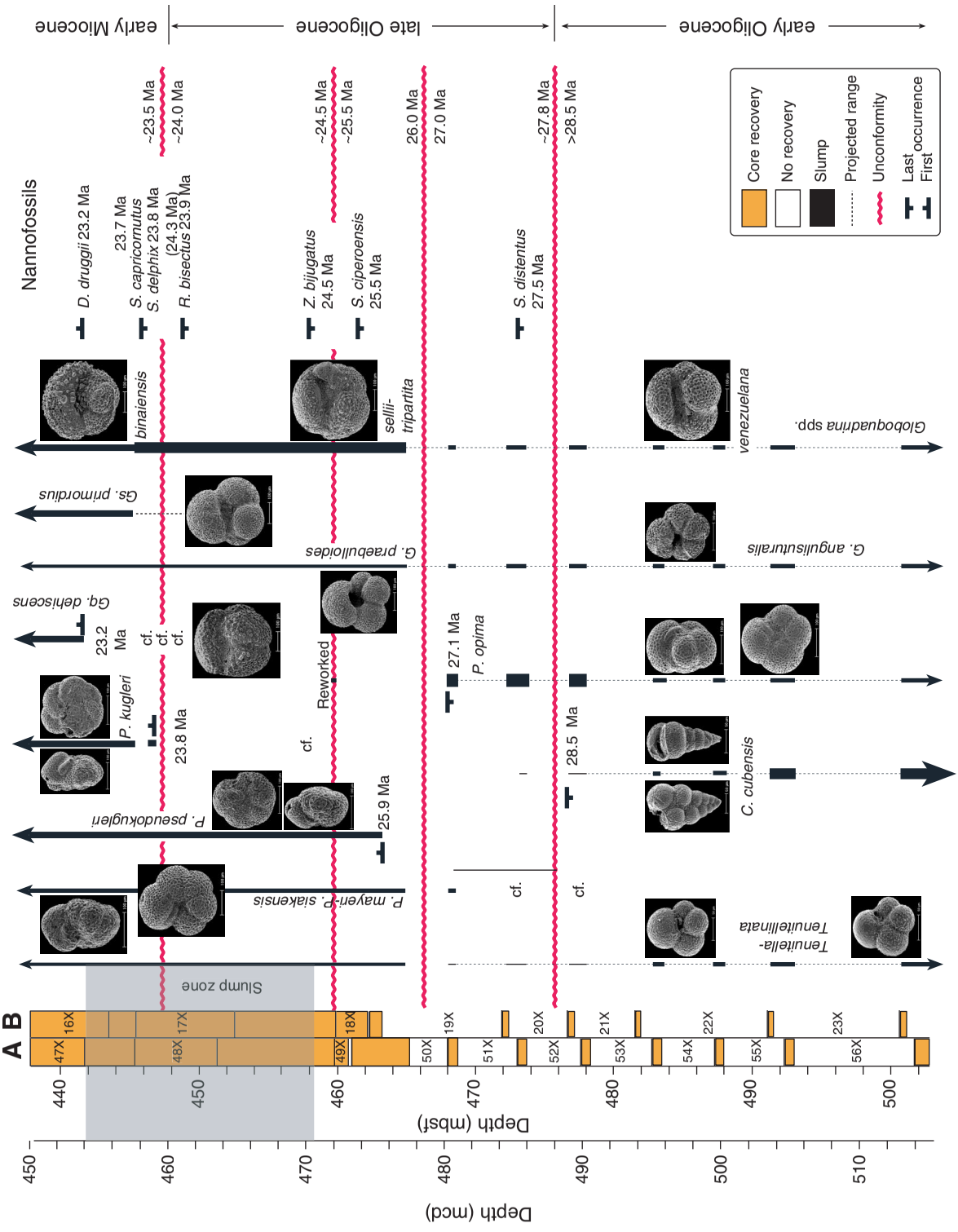

Figure F6. Determining upper Oligocene unconformities based on planktonic foraminifer and nannofossil datums.

Figure F7. Planktonic foraminifer zonation and inferred unconformities at Site 1148 and correlation between Sites 1146 and 1148. Site 1146 data are from Wang (2001).

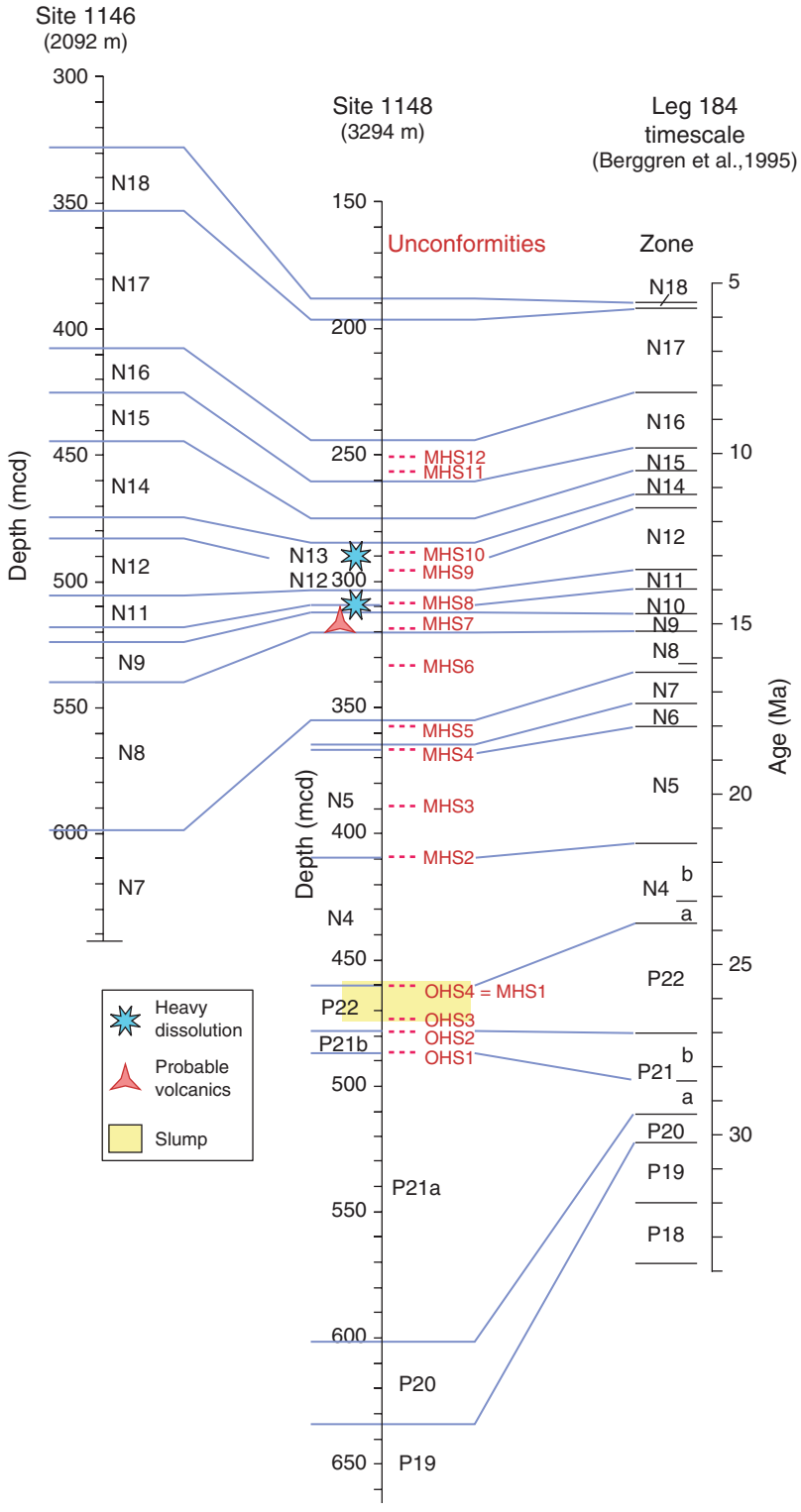

Figure F8. The biostratigraphic framework for Site 1148 (datum levels and sedimentation rates) on the basis of planktonic foraminifer, nannofossil, and isotopic datums given in Table T3, p. 25. The three local occurrences were adjusted: (1) LO of *Globoquadrina dehiscens*, (2) LO of *Globorotalia fohsi*, and (3) FO of *Globigerinatella insueta*. The lithostratigraphic units are from Wang, Prell, Blum, et al. (2000). Positions of unconformities and dissolution are indicated. Note the extremely high sedimentation rates in the early Oligocene.

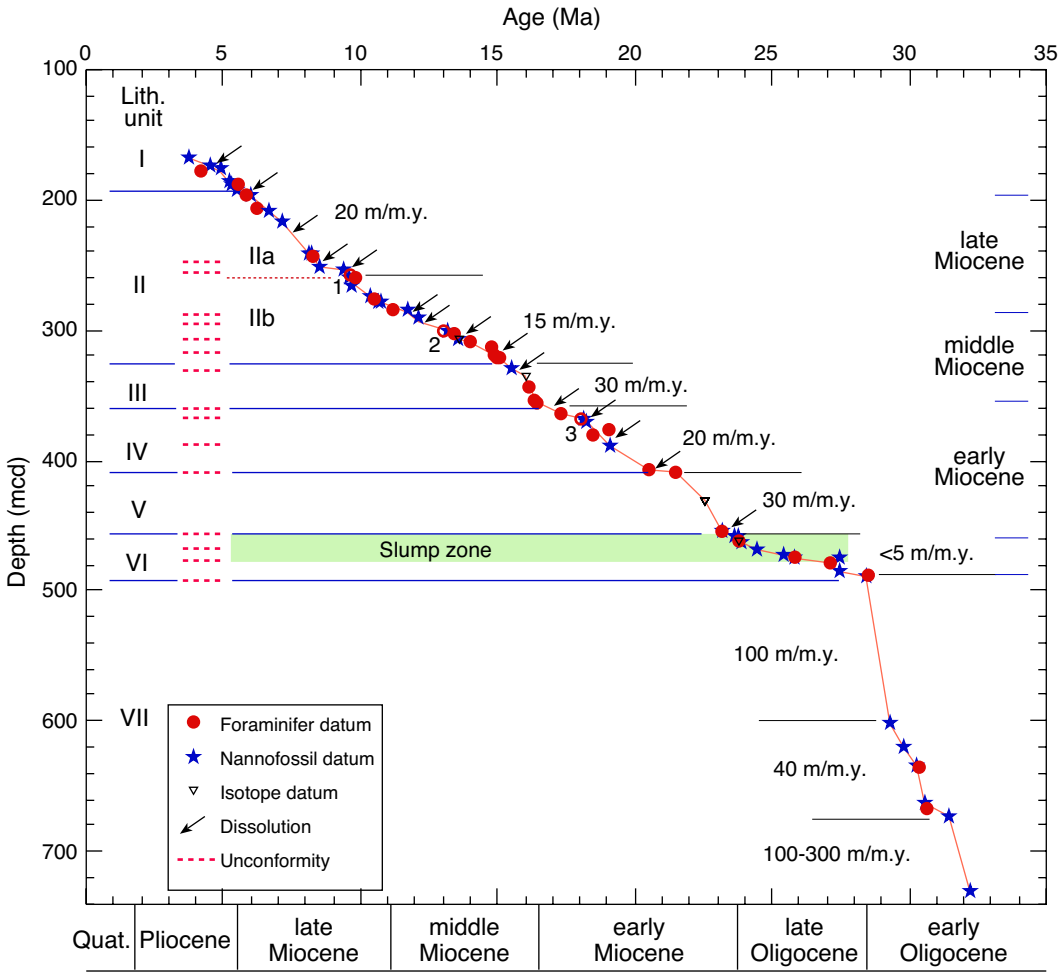

Figure F9. Sudden changes in color index and other physical property logs mark lithostratigraphic unit boundaries (Wang, Prell, Blum, et al., 2000). The carbonate content was measured by Chen et al. (2002). Most rapid swings in these parameters can be attributed to unconformities, at least for the Oligocene–Miocene interval.

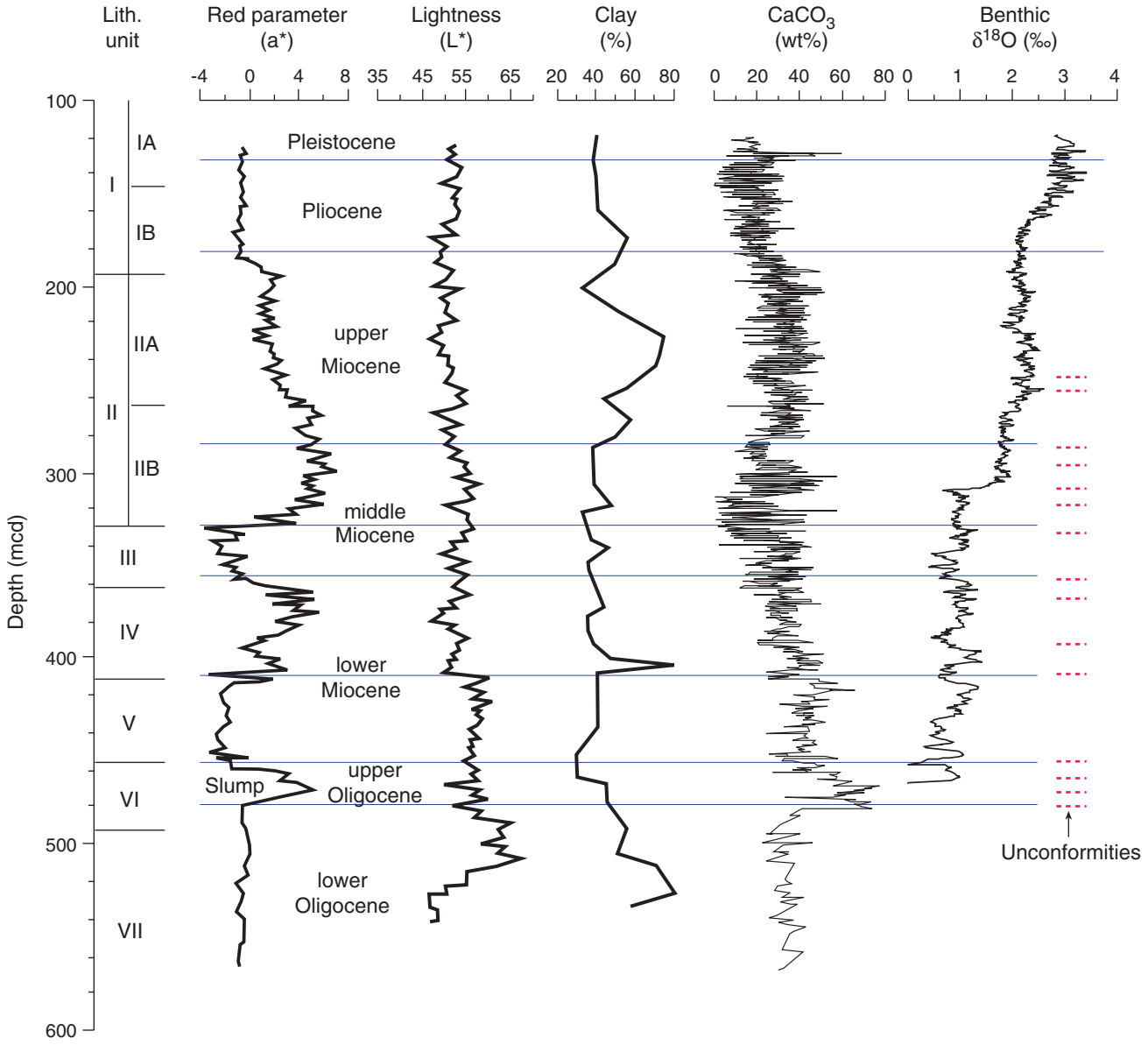

Figure F10. Lithobiostragraphic events recorded at Site 1148 manifest regional tectonic and third-order global paleoceanographic events (glacio-eustasy of Haq et al., 1987; sequences and MLi and MSi events of Hardenbol et al., 1998; Mi and Oi isotopic glaciations of Miller et al., 1991). Benthic oxygen isotope curve for Site 1148 was from Zhao et al. (2001).

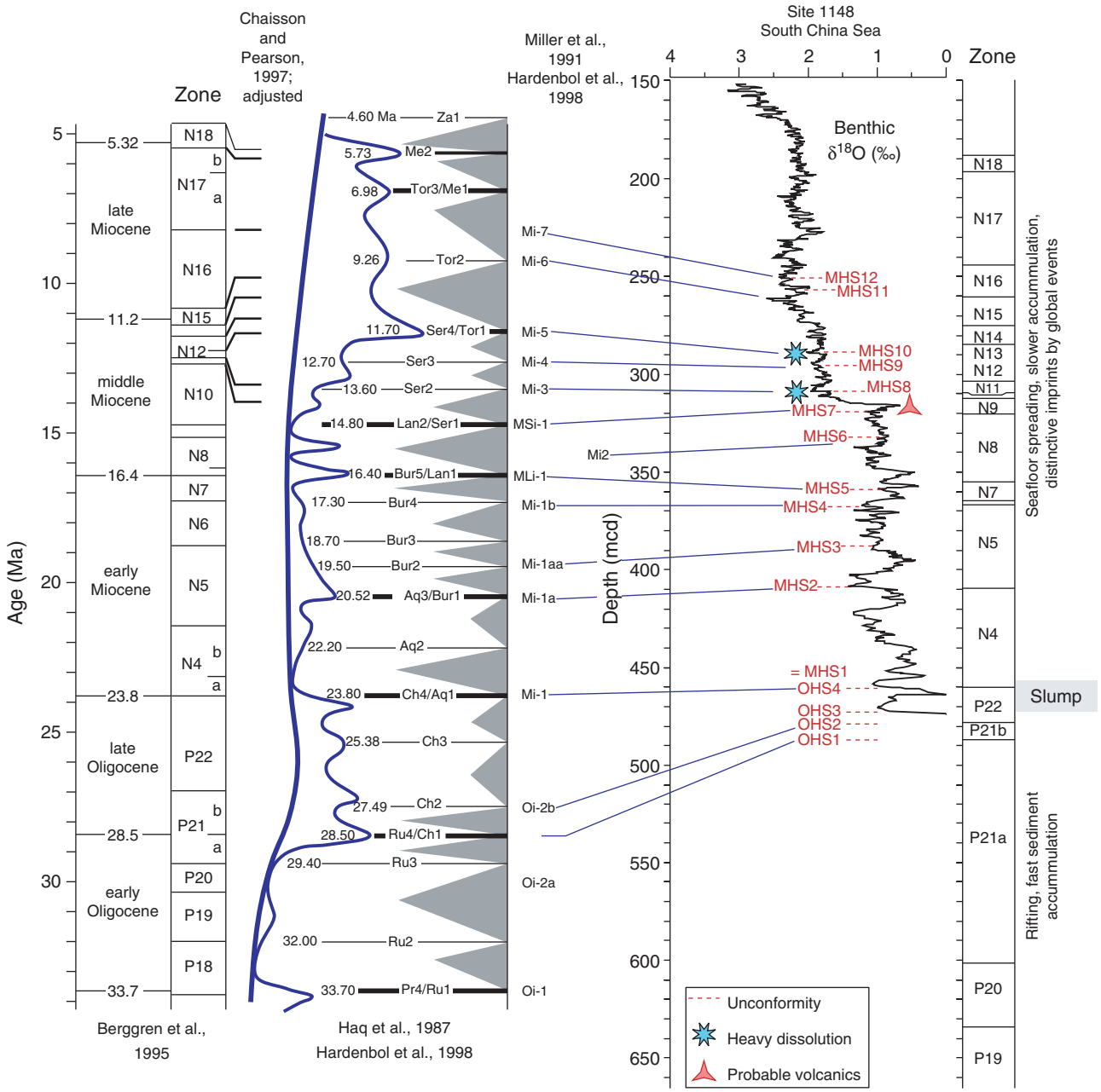

Table T1. Distribution of Miocene planktonic foraminifers, Site 1148 (This table is available in an **oversized format.**)

Table T2. Oligocene–Miocene planktonic foraminifer datum levels recognized at Site 1148.

Event	Top		Bottom		Mean depth (mcd)	Age (Ma)	Reference
	Core, section, interval (cm)	Depth (mcd)	Core, section, interval (cm)	Depth (mcd)			
	184-1148A-		184-1148A-				
LO *Globoturborotalita nepenthes*	19X-2, 60–62	176.83	19X-2, 75–77	176.98	176.91	4.20	Berggren et al., 1995
FO *Sphaeroidinella dehiscens*	20X-3, 75–77	189.08	20X-3, 90–92	188.23	188.16	5.54	Chaisson and Pearson, 1997
FO *Globorotalia tumida*	21X-2, 45–47	195.98	21X-2, 60–62	196.18	196.08	5.82	Chaisson and Pearson, 1997
FO *Globigerinoides conglobatus*	22X-2, 148–150	206.71	22X-3, 15–17	206.88	206.79	6.20	Chaisson and Pearson, 1997
FO *Globigerinoides extremus*	26X-2, 45–47	244.18	26X-2, 60–62	244.33	244.26	8.30	Berggren et al., 1995
LO *Globoquadrina dehiscens*	27X-4, 75–77	257.08	27X-4, 90–92	257.23	257.16	**9.5–9.8**	Site 1148 datum
FO *Neogloboquadrina acostaensis*	27X-6, 15–17	259.63	27X-6, 30–32	259.78	259.70	9.82	Chaisson and Pearson, 1997
LO *Paragloborotalia mayeri*	29X-3, 118–120	275.21	29X-3, 120–122	275.23	275.22	10.49	Chaisson and Pearson, 1997
FO *Globoturborotalita nepenthes*	30X-3, 0–2	283.63	30X-3, 30–32	283.93	283.78	11.19	Chaisson and Pearson, 1997
LO *Globorotalia fohsi*	32X-1, 117–119	301.00	32X-1, 120–122	301.03	301.02	**13.00**	Site 1148 datum
FO *Globorotalia fohsi*	32X-3, 30–32	303.13	32X-3, 60–62	303.43	303.28	13.42	Pearson and Chaisson, 1997
Mi-3					***309.28***	***13.60***	Miller et al., 1991, 1996
FO *Globorotalia praefohsi*	32X-6, 120–122	308.53	32X-7, 0–2	308.83	308.68	14.00	Pearson and Chaisson, 1997
LO *Praeorbulina glomerosa*	33X-2, 120–122	312.23	33X-3, 0–2	312.53	312.38	14.80	Berggren et al., 1995
FO *Globorotalia praemenardii*	33X-6, 90–92	317.93	33X-6, 120–122	318.23	317.98	14.90	Pearson and Chaisson, 1997
LO *Globigerinatella insueta*	34X-3, 0–2	320.82	34X-3, 30–32	321.12	320.97	15.00	Pearson and Chaisson, 1997
FO *Orbulina*	34X-2, 90–92	320.22	34X-2, 120–122	320.52	320.37	15.10	Berggren et al., 1995
Mi-2 (= CM3)					***337.23***	***16.0–16.2***	Mutti, 2000; Billups et al., 2002
FO *Globorotalia glomerosa*	36X-4, 120–122	344.13	36X-5, 0–2	344.43	344.18	16.10	Berggren et al., 1995
FO *Globorotalia curva*	37X-4, 30–32	352.83	37X-4, 60–62	353.13	352.98	16.30	Berggren et al., 1995
FO *Globorotalia sicana*	37X-5, 120–122	355.24	37X-6, 0–2	355.54	355.39	16.40	Berggren et al., 1995
LO *Catapsydrax dissimilis*	38X-5, 120–122	364.73	38X-6, 0–2	365.03	364.88	17.30	Berggren et al., 1995
FO *Globorotalia praescitula*	39X-CC, 26–33	374.74	40X-CC, 26–33	384.31	379.53	18.50	Wang, Prell, Blum, et al., 2000
FO *Globigerinatella insueta*	38X-CC, 30–32	367.30	39X-1, 30–32	367.43	367.37	**18.00**	Site 1148 datum
LO *Globoquadrina binaiensis*	40X-1, 30–32	377.03	40X-1, 60–62	377.33	377.18	19.10	Pearson and Chaisson, 1997
FO *Globigerinoides altiapertura*	43X-1, 45–47	406.18	43X-1, 85–87	406.58	406.38	20.50	Berggren et al., 1995
LO *Paragloborotalia kugleri*	43X-2, 45–47	407.68	43X-2, 85–87	408.08	408.83	21.50	Berggren et al., 1995
CM–O/M (top)					***432.38***	***22.60***	Hodell and Woodruff, 1994
FO *Globoquadrina dehiscens*	47X-7, 45–46	453.87	48X-1, 45–46	454.47	454.17	23.20	Berggren et al., 1995
CM–O/M (base)					***458.98***	***23.80***	Flower et al., 1997
FO *Paragloborotalia kugleri*	48X-4, 125–126	459.77	48X-5, 45–46	460.47	460.12	23.80	Berggren et al., 1995
FO *Paragloborotalia pseudokugleri*	50X-2, 85–86	475.57	50X-2, 125–126	475.97	475.77	25.90	Berggren et al., 1995
LO *Paragloborotalia opima*	50X-3, 45–46	476.67	51X-1, 15–16	480.37	478.52	27.10	Berggren et al., 1995
LO *Chiloguembelina cubensis*	52X-CC, 15–16	485.47	53X-1, 15–16	490.07	487.77	28.50	Berggren et al., 1995
FO *Globigerina angulisuturalis*	65X-CC, 27–34	593.63	66X-CC, 33–40	609.68	601.66	29.40	Berggren et al., 1995
LO *Turborotalia ampliapertura*	68X-CC, 24–31	629.65	69X-CC, 36–43	639.27	634.46	30.30	Berggren et al., 1995
FO *Paragloborotalia opima*	71X-CC, 37–43	658.54	72X-CC, 34–40	668.09	663.32	30.60	Berggren et al., 1995
LO *Pseudohastigerina*	74X-CC		75X-CC	696.94	692.26	32.00	Berggren et al., 1995

Notes: FO = first occurrence, LO = last occurrence. Ages for local datum levels are given in bold. Isotopic events (bold italic) are based on Miller et al. (1991, 1996) and Woodruff and Savin (1991), and their age estimates were calculated using the timescale of Berggren et al. (1995).

Table T3. Dating the Miocene planktonic foraminifer zonal boundaries.

Zonal boundary	Age by B95* (Ma)	Age by CP97† (Ma)	Age difference (Ma)	Site 1148 depth (mcd)	Site 1146 depth (mcd)
N18/N19	4.7	5.54	+0.84	188	328
N17/N18	5.6	5.82	+0.22	196	352
N16/N17	8.3	8.58	+0.28	244	408
N15/N16	10.9	9.82	–1.08	260	426
N14/N15	11.4	10.49	–0.91	275	445
N13/N14	11.8	11.19	–0.61	284	475
N12/N13	12.3	11.68	0.62	—	482
N11/N12	12.5	13.42	0.9	303	506
N10/N11	12.7	14	1.3	309	519
N9/N10	14.8	—	—	312	523
N8/N9	15.1	—	—	320	540
N7/N8	16.4	—	—	355	600
N6/N7	17.3	—	—	365	616
N5/N6	18.8	—	—	367‡	—
N4/N5	21.5	—	—	409	—
P22/N4	23.8	—	—	460	—

Notes: * = ages by Berggren et al. (1995), † = ages adjusted by Chaisson and Pearson (1997) and Pearson and Chaisson (1997). At Site 1148, the Zone N12/N13 boundary is undecided, and the Zone N6/N7 boundary at 367 mcd (‡) is estimated to be ~18 Ma on the local FO of *Globigerinatella insueta* (Table **T1,** p. 23). Site 1146 data are from Wang (2001).

Table T4. Datum levels used for plotting Figure F7, p. 19.

Planktonic foraminifer datum	Depth (mcd)	Age (Ma)	Nannofossil datum *Reticulofenestra*	Depth (mcd)	Age (Ma)
LO *Globoturborotalita nepenthes*	176.83	4.20	LO *Reticulofenestra pseudoumbilicus*	169.67	3.82
FO *Sphaeroidinella dehiscens*	189.08	5.54	LO *Amaurolithus* spp.	175.11	4.56
FO *Globorotalia tumida*	195.98	5.82	LO *Ceratolithus acutus*	177.77	4.99
FO *Globigerinoides conglobatus*	206.71	6.20	FO *Ceratolithus rugosus*	187.37	5.23
FO *Globigerinoides extremus*	244.18	8.30	LO *Triquetrorhabdulus rugosus*	190.37	5.34
LO *Globoquadrina dehiscens*	257.08	*9.5-9.8*	FO *Ceratolithus acutus*	190.37	5.37
FO *Neogloboquadrina acostaensis*	259.63	9.82	LO *Discoaster quinqueramus*	193.31	5.54
LO *Paragloborotalia mayeri*	275.21	10.49	LO *Amaurolithus amplificus*	198.57	5.99
FO *Globoturborotalita nepenthes*	283.63	11.19	FO *Amaurolithus amplificus*	211.27	6.76
LO *Globorotalia fohsi*	301.00	*13.00*	FO *Amaurolithus primus*	219.37	7.24
FO *Globorotalia fohsi*	303.13	13.42	FO *Discoaster berggrenii*	242.61	8.20
Mi-2	***337.23***	***13.60***	FO *Discoaster quinqueramus*	242.61	8.28
FO *Globorotalia praefohsi*	308.53	14.00	FO *Discoaster pentaradiatus*	253.37	8.55
LO *Praeorbulina glomerosa*	312.23	14.80	LO *Discoaster hamatus*	256.37	9.40
FO *Globorotalia praemenardii*	317.93	14.90	LO *Catinaster calyculus*	261.81	9.64
LO *Globigerinatella insueta*	320.82	15.00	LO *Catinaster coalitus*	267.47	9.69
FO *Orbulina*	320.22	15.10	FO *Discoaster hamatus*	275.57	10.38
Mi-2 (= CM3)	***337.23***	***16.00***	FO *Catinaster calyculus*	279.21	10.70
FO *Globorotalia glomerosa*	344.13	16.10	FO *Catinaster coalitus*	281.01	10.79
FO *Globorotalia curva*	352.83	16.30	LO *Discoaster kugleri*	286.67	11.80
FO *Globorotalia sicana*	355.24	16.40	FO *Discoaster kugleri*	293.27	12.20
LO *Catapsydrax dissimilis*	364.73	17.30	FO *Triquetrorhabdulus rugosus*	302.87	13.20
FO *Globorotalia praescitula*	374.74	18.50	LO *Cyclicargolithus floridanus*	302.87	13.20
FO *Globigerinatella insueta*	367.30	18.00	LO *Sphenolithus heteromorphus*	308.81	13.57
LO *Globoquadrina binaiensis*	377.03	19.10	LO *Helicosphaera ampliaperta*	331.87	15.60
FO *Globigerinoides altiapertura*	406.18	20.50	FO *Sphenolithus heteromorphus*	370.17	18.20
LO *Paragloborotalia kugleri*	407.68	21.50	LO *Sphenolithus belemnos*	371.57	18.30
CM–O/M (top)	***432.38***	***22.60***	FO *Sphenolithus belemnos*	390.97	19.20
FO *Globoquadrina dehiscens*	453.87	23.20	FO *Discoaster druggii*	454.41	23.20
CM–O/M (base)	***458.98***	***23.80***	LO *Sphenolithus capricornutus*	458.57	23.70
FO *Paragloborotalia kugleri*	459.77	23.80	LO *Sphenolithus delphix*	458.57	23.80
FO *Paragloborotalia pseudokugleri*	475.57	25.90	LO *Dictyococcites bisectus*	461.57	23.90
LO *Paragloborotalia opima*	476.67	27.10	LO *Zygrhablithus bijugatus*	468.92	24.50
LO *Chiloguembelina cubensis*	485.47	28.50	LO *Sphenolithus ciperoensis*	473.61	25.50
FO *Globigerina angulisuturalis*	593.63	29.40	LO *Sphenolithus distentus*	485.34	27.50
LO *Turborotalia ampliapertura*	629.65	30.30	FO *Sphenolithus ciperoensis*	620.99	29.90
FO *Paragloborotalia opima*	658.54	30.60	FO *Sphenolithus distentus*	673.41	31.50
LO *Pseudohastigerina*	687.58	32.00	LO *Reticulofenestra umbilicus–Reticulofenestra hillae*	730.33	32.30

Notes: FO = first occurrence, LO = last occurrence. Planktonic foraminifer datums and isotopic events from Table T1, p. 23; nannofossil datums from Xin Su (pers. comm., 2002). Bold italic = isotopic events.